Supplemental Material to "Edge and corner skin effects of chirally coupled magnons characterized by a topological winding tuple"

Chengyuan Cai,[1] Dante M. Kennes,[2,3] Michael A. Sentef,[4,3] and Tao Yu[1,*]

[1] *School of Physics, Huazhong University of Science and Technology, Wuhan 430074, China*

[2] *Institut für Theorie der Statistischen Physik, RWTH Aachen University and JARA-Fundamentals of Future Information Technology, 52056 Aachen, Germany*

[3] *Max Planck Institute for the Structure and Dynamics of Matter, Luruper Chaussee 149, 22761 Hamburg, Germany*

[4] *Institute for Theoretical Physics and Bremen Center for Computational Materials Science, University of Bremen, 28359 Bremen, Germany*

(Dated: September 25, 2023)

I. MAGNETIC CONFIGURATION

The magnetic array composed of small nanomagnets of width w, length l, and thickness d is uniformly distributed on a finite area of the magnetic substrate of thickness s, as illustrated in Fig. S1. The distance between neighboring nanomagnet is Λ_y and Λ_z, respectively, in the $\hat{\mathbf{y}}$ and $\hat{\mathbf{z}}$ directions. There are N_z rows and N_y columns in the array. We number (a, b) for the nanomagnet in the a-th column and b-th row.

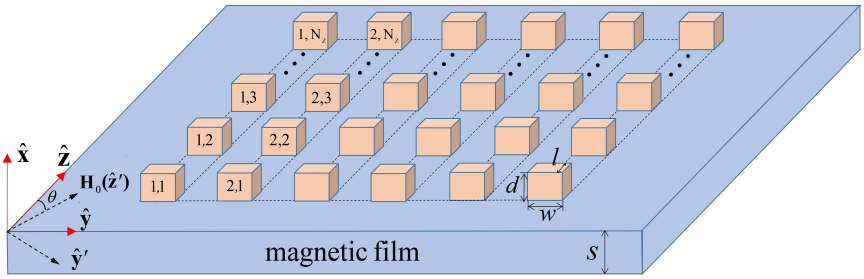

FIG. S1. Two-dimensional magnetic array fabricated on a finite area of a magnetic substrate.

An in-plane magnetic field $\mathbf{H}_0$ with an angle θ with respect to the $\hat{\mathbf{z}}$-direction is applied, which biases the magnetization of the substrate to be parallel. On the other hand, the magnetization $\tilde{\mathbf{M}}_s$ in the nanomagnet follows $\mathbf{H}_0$ with an angle $\tilde{\theta}$ with respect to the $\hat{\mathbf{z}}$ direction [Fig. S2(a)] that we resolve in the following.

The magnetization direction of the nanomagnet at equilibrium is governed by the free-energy density

$$\begin{aligned} F_m &= -\mu_0 \tilde{\mathbf{M}}_s \cdot \mathbf{H}_0 + \frac{\mu_0}{2} N_{zz} \tilde{M}_z^2 + \frac{\mu_0}{2} N_{yy} \tilde{M}_y^2 \\ &= -\mu_0 \tilde{M}_s H_0 \cos\left(\theta - \tilde{\theta}\right) + \frac{\mu_0}{2} N_{zz} \tilde{M}_s^2 \cos^2\tilde{\theta} + \frac{\mu_0}{2} N_{yy} \tilde{M}_s^2 \sin^2\tilde{\theta}, \end{aligned} \tag{S1}$$

* taoyuphy@hust.edu.cn

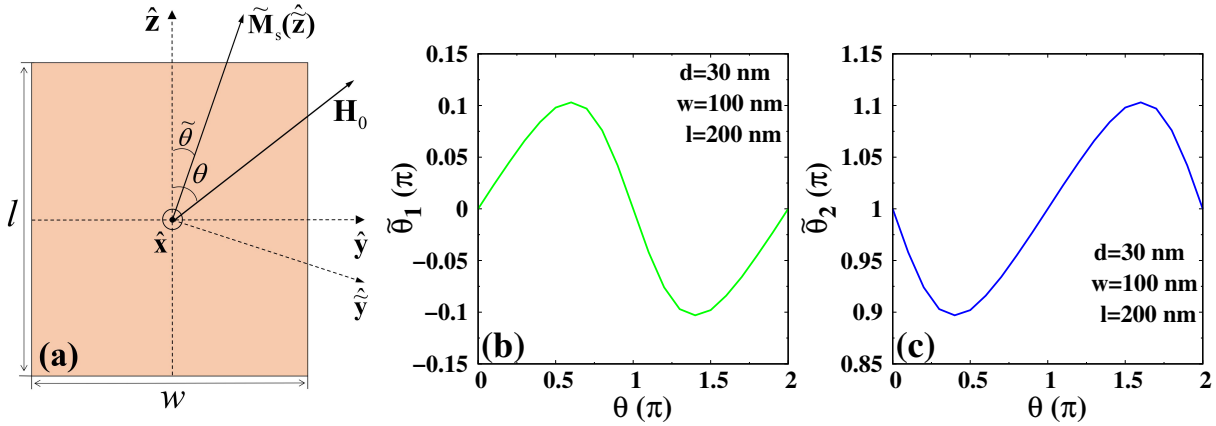

FIG. S2. (a) shows the top view of a nanomagnet. $\mathbf{H}_0$ is the applied magnetic field and $\tilde{\mathbf{M}}_s$ is the saturated magnetization of the nanomagnet. (b) and (c) plot the dependence of the direction of $\tilde{\mathbf{M}}_s$ on the field direction θ. Two configurations with $\tilde{\theta}_1$ and $\tilde{\theta}_2$ are all stable when the bias field is small.

where the demagnetization factors

$$N_{xx} \simeq \frac{wl}{wl+wd+ld}, \quad N_{yy} \simeq \frac{ld}{wl+wd+ld}, \quad N_{zz} \simeq \frac{wd}{wl+wd+ld}. \tag{S2}$$

The configuration with minimum free energy, i.e., $dF_m/d\tilde{\theta} = 0$ and $d^2F_m/d\tilde{\theta}^2 > 0$, is stable:

$$H_0 \sin\left(\theta - \tilde{\theta}\right) + (\tilde{M}_s/2)(N_{zz} - N_{yy}) \sin\left(2\tilde{\theta}\right) = 0, \tag{S3a}$$

$$H_0 \cos\left(\theta - \tilde{\theta}\right) - \tilde{M}_s(N_{zz} - N_{yy}) \cos\left(2\tilde{\theta}\right) > 0. \tag{S3b}$$

For $\mu_0\tilde{M}_s = 1.6$ T [1] of CoFeB and $\mu_0 H_0 = 0.05$ T, there are two stable magnetic configurations $\tilde{\theta}_1$ and $\tilde{\theta}_2$ for the nanomagnet with $d = 30$ nm, $w = 100$ nm, and $l = 200$ nm, which we numerically calculate in Fig. S2(b) and (c).

II. CHIRAL DIPOLAR COUPLING BETWEEN MAGNONS

We focus on the Kittle mode of the nanomagnet. The effective magnetic field $\mathbf{H}_{\text{eff}}$, in the lab $\{x, y, z\}$-coordinate system, is mainly contributed by the applied magnetic field $\mathbf{H}_0$ and the demagnetization field $\mathbf{H}_d$:

$$\mathbf{H}_{\text{eff}} = \mathbf{H}_0 + \mathbf{H}_d = \begin{pmatrix} -N_{xx}\tilde{M}_x \\ -N_{yy}\tilde{M}_y + H_0 \sin\tilde{\theta} \\ -N_{zz}\tilde{M}_z + H_0 \cos\tilde{\theta} \end{pmatrix}. \tag{S4}$$

In order to calculate the eigenmode in the nanomagnet, we transform to the local $\{\tilde{x}, \tilde{y}, \tilde{z}\}$-coordinate system, where the $\hat{\tilde{\mathbf{z}}}$-axis is along $\tilde{\mathbf{M}}_s$ and the $\hat{\tilde{\mathbf{x}}}$-axis is normal to the substrate as shown in Fig. S2(a). We transform from the lab system to the local system in terms of the rotation matrix

$$\tilde{\mathcal{R}}(\tilde{\theta}) = \begin{pmatrix} 1 & 0 & 0 \\ 0 & \cos\tilde{\theta} & -\sin\tilde{\theta} \\ 0 & \sin\tilde{\theta} & \cos\tilde{\theta} \end{pmatrix}. \tag{S5}$$

The components of the magnetic field and magnetization transform according to $\tilde{H}_{\tilde{\mu}} = \tilde{\mathcal{R}}_{\tilde{\mu}\nu} H_\nu$ and $\tilde{M}_\mu = \tilde{\mathcal{R}}^{-1}_{\mu\tilde{\nu}} \tilde{M}_{\tilde{\nu}}$, leading to

$$\begin{pmatrix} H_{\tilde{x}} \\ H_{\tilde{y}} \\ H_{\tilde{z}} \end{pmatrix} = \begin{pmatrix} -N_{xx}\tilde{M}_{\tilde{x}} \\ -(N_{yy}\cos^2\tilde{\theta} + N_{zz}\sin^2\tilde{\theta})\tilde{M}_{\tilde{y}} \\ (N_{zz}-N_{yy})\sin\tilde{\theta}\cos\tilde{\theta}\tilde{M}_{\tilde{y}} - (N_{yy}\sin^2\tilde{\theta} + N_{zz}\cos^2\tilde{\theta})\tilde{M}_{\tilde{z}} + H_0\cos\Big(\theta-\tilde{\theta}\Big) \end{pmatrix}. \tag{S6}$$

The magnetization $\tilde{\mathbf{M}}$ of the nanomagnet obeys the Landau-Lifshitz (LL) equation, which in the linear regime reads

$$\begin{aligned} \frac{\partial \tilde{M}_{\tilde{x}}}{\partial t} &= -\mu_0\gamma\left[H_0\cos\Big(\theta-\tilde{\theta}\Big) - \tilde{M}_s(\cos^2\tilde{\theta}-\sin^2\tilde{\theta})(N_{zz}-N_{yy})\right]\tilde{M}_{\tilde{y}}, \\ \frac{\partial \tilde{M}_{\tilde{y}}}{\partial t} &= \mu_0\gamma\left[H_0\cos\Big(\theta-\tilde{\theta}\Big) - \tilde{M}_s(N_{yy}\sin^2\tilde{\theta} + N_{zz}\cos^2\tilde{\theta} - N_{xx})\right]\tilde{M}_{\tilde{x}}, \end{aligned} \tag{S7}$$

where μ_0 is the vacuum permeability, and γ is the modulus of the electron gyromagnetic ratio. We obtain the FMR frequency $\Omega = \sqrt{\omega_1\omega_2}$ and the ratio $\tilde{M}_{\tilde{y}}/\tilde{M}_{\tilde{x}} = i\xi_m^2 = i\omega_2/\omega_1$ for the Kittel mode, where

$$\begin{aligned} \omega_1 &= \mu_0\gamma\left(H_0\cos\Big(\theta-\tilde{\theta}\Big) - \tilde{M}_s(\cos^2\tilde{\theta}-\sin^2\tilde{\theta})(N_{zz}-N_{yy})\right), \\ \omega_2 &= \mu_0\gamma\left(H_0\cos\Big(\theta-\tilde{\theta}\Big) - \tilde{M}_s(N_{yy}\sin^2\tilde{\theta} + N_{zz}\cos^2\tilde{\theta} - N_{xx})\right). \end{aligned} \tag{S8}$$

Via the normalization condition $\int d\mathbf{r}\left(\tilde{\mathcal{M}}_{\tilde{x}}\tilde{\mathcal{M}}^*_{\tilde{y}} - \tilde{\mathcal{M}}^*_{\tilde{x}}\tilde{\mathcal{M}}_{\tilde{y}}\right) = -i/2$, the normalized eigenmodes $\tilde{\mathcal{M}}_{\tilde{x}} = -1/\left(2\xi_m\sqrt{lwd}\right)$ and $\tilde{\mathcal{M}}_{\tilde{y}} = -i\xi_m/\left(2\sqrt{lwd}\right)$, with which the magnetization in the (a,b)-th nanomagnet is quantized in terms of the magnon operators $\hat{\beta}_{a,b}$:

$$\hat{\tilde{M}}^{(a,b)}_{\alpha=\{\tilde{x},\tilde{y}\}}(\mathbf{r}) = -\sqrt{2\tilde{M}_s\gamma\hbar}\tilde{\mathcal{M}}_\alpha\hat{\beta}_{a,b} + \text{H.c.}. \tag{S9}$$

We transform back to the lab $\{x,y,z\}$-coordinate system by $\tilde{M}_\mu = \tilde{\mathcal{R}}^{-1}_{\mu\tilde{\nu}}\tilde{M}_{\tilde{\nu}}$:

$$\hat{\tilde{M}}^{(a,b)}_x(\mathbf{r}) = -\sqrt{2\tilde{M}_s\gamma\hbar}\left(\tilde{\mathcal{M}}_{\tilde{x}}\hat{\beta}_{a,b} + \text{H.c.}\right), \tag{S10a}$$

$$\hat{\tilde{M}}^{(a,b)}_y(\mathbf{r}) = -\sqrt{2\tilde{M}_s\gamma\hbar}\left(\tilde{\mathcal{M}}_{\tilde{y}}\hat{\beta}_{a,b} + \text{H.c.}\right)\cos\tilde{\theta} + \sin\tilde{\theta}\tilde{M}_s, \tag{S10b}$$

$$\hat{\tilde{M}}^{(a,b)}_z(\mathbf{r}) = -\sqrt{2\tilde{M}_s\gamma\hbar}\left(\tilde{\mathcal{M}}_{\tilde{y}}\hat{\beta}_{a,b} + \text{H.c.}\right)\sin\tilde{\theta} + \cos\tilde{\theta}\tilde{M}_s. \tag{S10c}$$

For the magnetic substrate, the equilibrium magnetization $\mathbf{M}_s$ is along $\mathbf{H}_0$. We consider the dynamics of $\mathbf{M}$ in the local $\{x',y',z'\}$-coordinate system, where the $\hat{\mathbf{z}}'$-axis is along $\mathbf{H}_0$ and the $\hat{\mathbf{x}}'$-axis is normal to the substrate (Fig. S1). From the LL equation, we obtain the eigenfrequency of the spin wave of wave vector $\mathbf{k}'$

$$\omega(\mathbf{k}') = \mu_0\gamma(H_0 + \alpha_{\text{ex}}M_s k'^2), \tag{S11}$$

and the normalized amplitudes $\mathcal{M}_{x'} = -1/(2\sqrt{L_yL_zs})$ and $\mathcal{M}_{y'} = -i/(2\sqrt{L_yL_zs})$, where α_{ex} is the exchange stiffness of the substrate, and L_y and L_z are the lengths of substrate along the $\hat{\mathbf{y}}$- and $\hat{\mathbf{z}}$-directions. With the magnon annihilation operator $\hat{m}_{\mathbf{k}'}$, the magnetization operator $\hat{\mathbf{M}}(\mathbf{r}')$ of the substrate in the linear regime is quantized by

$$\begin{aligned} \hat{M}_{z'}(\mathbf{r}') &= M_s, \\ \hat{M}_{\beta=\{x',y'\}}(\mathbf{r}') &= -\sqrt{2M_s\gamma\hbar}\sum_{\mathbf{k}'}\left(\mathcal{M}_\beta e^{i\mathbf{k}'\cdot\boldsymbol{\rho}'}\hat{m}_{\mathbf{k}'} + \text{H.c.}\right), \end{aligned} \tag{S12}$$

where the inplane $\boldsymbol{\rho}' = y'\hat{\mathbf{y}}' + z'\hat{\mathbf{z}}'$. To facilitate the calculation of the coupling between the magnons in the nanomagnet and substrate, we transform back to the lab $\{x, y, z\}$-coordinate system by a counterclockwise rotation of θ with respect to the $\hat{\mathbf{x}}$-axis in terms of the rotation matrix

$$\mathcal{R}(\theta) = \begin{pmatrix} 1 & 0 & 0 \\ 0 & \cos\theta & \sin\theta \\ 0 & -\sin\theta & \cos\theta \end{pmatrix}. \tag{S13}$$

The components of the magnetization and the wave vector in Eq. (S12) transform according to $M_\mu(r_\alpha) = \mathcal{R}_{\mu\nu'} M_{\nu'}(\mathcal{R}^{-1}_{\alpha\beta'} r_{\beta'})$ and $k_\mu = \mathcal{R}_{\mu\nu'} k_{\nu'}$, leading to the magnetization operator in the lab $\{x, y, z\}$-coordinate system

$$\hat{M}_x(\mathbf{r}) = -\sqrt{2M_s\gamma\hbar}\sum_{\mathbf{k}} \left(\mathcal{M}_{x'} e^{i\mathbf{k}\cdot\boldsymbol{\rho}} \hat{m}_{\mathbf{k}} + \text{H.c.}\right), \tag{S14a}$$

$$\hat{M}_y(\mathbf{r}) = -\sqrt{2M_s\gamma\hbar}\sum_{\mathbf{k}} \left(\mathcal{M}_{y'} e^{i\mathbf{k}\cdot\boldsymbol{\rho}} \hat{m}_{\mathbf{k}} + \text{H.c.}\right)\cos\theta + \sin\theta M_s, \tag{S14b}$$

$$\hat{M}_z(\mathbf{r}) = \sqrt{2M_s\gamma\hbar}\sum_{\mathbf{k}} \left(\mathcal{M}_{y'} e^{i\mathbf{k}\cdot\boldsymbol{\rho}} \hat{m}_{\mathbf{k}} + \text{H.c.}\right)\sin\theta + \cos\theta M_s. \tag{S14c}$$

The spin wave of the substrate generates a dipolar field above it

$$\hat{\mathbf{h}}(\mathbf{r}) = -\sqrt{2M_s\gamma\hbar}\sum_{\mathbf{k}} \frac{e^{-kx} - e^{-k(x+s)}}{2k^2} \left(\sin\theta k_z \mathcal{M}_{y'} - \cos\theta k_y \mathcal{M}_{y'} - ik\mathcal{M}_{x'}\right) \begin{pmatrix} ik \\ k_y \\ k_z \end{pmatrix} e^{i\mathbf{k}\cdot\boldsymbol{\rho}} \hat{m}_{\mathbf{k}} + \text{H.c.}, \tag{S15}$$

where $k = \sqrt{k_y^2 + k_z^2}$ is the magnitude of $\mathbf{k}$. For the (a, b)-th nanomagnet located at the center position $(d/2, a\Lambda_y, b\Lambda_z)$, its Kittel magnon couples via the dipolar interaction with the magnon in the substrate

$$\begin{aligned} \hat{H}_c &= -\mu_0 \sum_{a,b} \int_0^d dx \int_{a\Lambda_y - w/2}^{a\Lambda_y + w/2} dy \int_{b\Lambda_z - l/2}^{b\Lambda_z + l/2} dz \hat{\mathbf{h}}(\mathbf{r}) \cdot \hat{\tilde{\mathbf{M}}}^{(a,b)}(\mathbf{r}) \\ &= \sum_{a,b}\sum_{\mathbf{k}} \hbar g_{\mathbf{k}}^{(a,b)} \hat{m}_{\mathbf{k}} \hat{\beta}_{a,b}^\dagger + \text{H.c.}, \end{aligned} \tag{S16}$$

in which the coupling constant

$$\begin{aligned} g_{\mathbf{k}}^{(a,b)} &= -4\mu_0\gamma\sqrt{M_s\tilde{M}_s} \frac{\left(1 - e^{-kd}\right)\left(1 - e^{-ks}\right)}{k^3 k_y k_z} \sin\left(\frac{k_y w}{2}\right) \sin\left(\frac{k_z l}{2}\right) e^{i(ak_y\Lambda_y + bk_z\Lambda_z)} \\ &\times (\mathcal{M}_{x'}, \mathcal{M}_{y'}) \begin{pmatrix} k^2 & -ik(k_y\cos\tilde{\theta} - k_z\sin\tilde{\theta}) \\ ik(k_z\sin\theta - k_y\cos\theta) & (k_z\sin\theta - k_y\cos\theta)(k_y\cos\tilde{\theta} - k_z\sin\tilde{\theta}) \end{pmatrix} \begin{pmatrix} \tilde{\mathcal{M}}_{\tilde{x}}^* \\ \tilde{\mathcal{M}}_{\tilde{y}}^* \end{pmatrix} \\ &= g_{\mathbf{k}} e^{i(ak_y\Lambda_y + bk_z\Lambda_z)}, \end{aligned} \tag{S17}$$

where $g_{\mathbf{k}}$ is a real number.

III. EFFECTIVE MAGNON HAMILTONIAN OF NANOMAGNET SUBSYSTEM

We construct the effective Hamiltonian of the magnons in the nanomagnets by integrating the degree of freedom of the substrate. The total Hamiltonian

$$\hat{H} = \sum_{a,b} \hbar(\Omega - i\delta_\beta) \hat{\beta}_{a,b}^\dagger \hat{\beta}_{a,b} + \sum_{\mathbf{k}} \hbar(\omega_k - i\delta_m) \hat{m}_{\mathbf{k}}^\dagger \hat{m}_{\mathbf{k}} + \left(\sum_{a,b}\sum_{\mathbf{k}} \hbar g_{\mathbf{k}}^{(a,b)} \hat{m}_{\mathbf{k}} \hat{\beta}_{a,b}^\dagger + \text{H.c.}\right), \tag{S18}$$

where $\delta_\beta \approx \tilde{\alpha}_G\Omega$ and $\delta_m(k) \approx \alpha_G\omega_k$ with $\tilde{\alpha}_G$ and α_G denoting, respectively, the Gilbert damping constants for the nanomagnet and substrate. The Langevin's equations of $\hat{\beta}_{(a,b)}$ and $\hat{m}_{\mathbf{k}}$ in the frequency domain read

$$(\omega - \omega_k + i\delta_m)\,\hat{m}_{\mathbf{k}}(\omega) = \sum_{a,b} e^{-i(ak_y\Lambda_y + bk_z\Lambda_z)} g_{\mathbf{k}}\hat{\beta}_{a,b}(\omega), \tag{S19a}$$

$$(\omega - \Omega + i\delta_\beta)\,\hat{\beta}_{a,b}(\omega) = \sum_{\mathbf{k}} e^{i(ak_y\Lambda_y + bk_z\Lambda_z)} g_{\mathbf{k}}\hat{m}_{\mathbf{k}}(\omega), \tag{S19b}$$

from which we find

$$\hat{m}_{\mathbf{k}}(\omega) = \sum_{a,b} \frac{e^{-i(ak_y\Lambda_y + bk_z\Lambda_z)} g_{\mathbf{k}}}{\omega - \omega_{\mathbf{k}} + i\delta_m}\hat{\beta}_{a,b}. \tag{S20}$$

Substituting into Eq. (S19b), we find

$$(\omega - \Omega + i\delta_\beta)\,\hat{\beta}_{a,b} = \sum_{a',b'}\sum_{\mathbf{k}} \frac{e^{i\left[(a-a')k_y\Lambda_y + (b-b')k_z\Lambda_z\right]}}{\omega - \omega_{\mathbf{k}} + i\delta_m} g_{\mathbf{k}}^2\hat{\beta}_{a',b'}. \tag{S21}$$

The magnons in the substrate mediate an effective interaction between Kittel magnons in the nanomagnet.

Since $\omega_k = \mu_0\gamma(H_0 + \alpha_{\rm ex}M_s k^2)$ only depends on the magnitude of $\mathbf{k}$, the summation over $\mathbf{k}$ in Eq. (S21) is conveniently performed in the polar $\{k, \varphi\}$-coordinate:

$$\begin{aligned}
&\sum_{a',b'}\sum_{\mathbf{k}} \frac{e^{i\left[(a-a')k_y\Lambda_y + (b-b')k_z\Lambda_z\right]}}{\omega - \omega_k + i\delta_m} g_{\mathbf{k}}^2\hat{\beta}_{a',b'} \\
&= \frac{L_yL_z}{(2\pi)^2}\sum_{a',b'}\int_0^{2\pi} d\varphi \int_0^{\infty} dk \frac{kg^2(k,\varphi)}{\omega - \omega_k + i\delta_m} e^{ik\left((a-a')\cos\varphi\Lambda_y + (b-b')\sin\varphi\Lambda_z\right)}\hat{\beta}_{a',b'} \\
&= \frac{L_yL_z}{(2\pi)^2}\sum_{a',b'}\int_0^{\pi} d\varphi \int_{-\infty}^{\infty} dk \frac{|k|g^2(k,\varphi)}{\omega - \omega_k + i\delta_m} e^{ikr_{a-a',b-b'}\cos\left(\varphi - \phi_{a-a',b-b'}\right)}\hat{\beta}_{a',b'},
\end{aligned} \tag{S22}$$

where we define $\mathbf{r}_{a-a',b-b'} = (a-a')\Lambda_y\hat{\mathbf{y}} + (b-b')\Lambda_z\hat{\mathbf{z}}$ in the polar coordinate with magnitude $r_{a-a',b-b'}$ and polar angle $\phi_{a-a',b-b'}$. When $a = a'$ and $b = b'$ or $\varphi = \pm\pi/2 + \phi_{a-a',b-b'}$,

$$\begin{aligned}
\frac{L_yL_z}{(2\pi)^2}\int_0^{\pi} d\varphi \int_{-\infty}^{\infty} dk \frac{|k|g^2(k,\varphi)}{\omega - \omega_k + i\delta_m}\hat{\beta}_{a',b'} &= -i\frac{L_yL_z}{4\pi}\int_0^{\pi} d\varphi \left(\frac{k_\omega}{v_{k_\omega}}g^2(k_\omega,\varphi) + \frac{-k_\omega}{-v_{k_\omega}}g^2(-k_\omega,\varphi)\right)\hat{\beta}_{a',b'} \\
&= -i\frac{L_yL_z}{4\pi}\int_0^{\pi} d\varphi \left(\frac{k_\omega}{v_{k_\omega}}g^2(k_\omega,\varphi) + \frac{k_\omega}{v_{k_\omega}}g^2(k_\omega,\pi+\varphi)\right)\hat{\beta}_{a',b'} \\
&= -i\frac{L_yL_z}{4\pi}\int_0^{2\pi} d\varphi \frac{k_\omega}{v_{k_\omega}}g^2(k_\omega,\varphi)\hat{\beta}_{a',b'},
\end{aligned} \tag{S23}$$

where $k_\omega = \sqrt{(\omega - \mu_0\gamma H_0)/(\mu_0\gamma\alpha_{\rm ex}M_s)}$, and $v_{k_\omega} = (\partial\omega_k/\partial k)|_{k_\omega} = 2\mu_0\gamma\alpha_{\rm ex}M_s k_\omega$. Otherwise, $r_{a-a',b-b'} > 0$. For $(\varphi - \phi_{a-a',b-b'}) \in (-\pi/2, \pi/2)$, $\cos(\varphi - \phi_{a-a',b-b'}) > 0$, so we close the contour integration in the upper complex plane, where the singularity is located at $q_\omega = k_\omega(1 + i\alpha_G/2)$, leading to

$$\int_{-\infty}^{\infty} dk \frac{e^{ikr_{a-a',b-b'}\cos\left(\varphi - \phi_{a-a',b-b'}\right)}|k|g^2(k,\varphi)}{\omega - \omega_k + i\delta_m} = -2\pi i\frac{k_\omega}{v_{k_\omega}}g^2(k_\omega,\varphi)e^{iq_\omega r_{a-a',b-b'}\cos\left(\varphi - \phi_{a-a',b-b'}\right)}. \tag{S24}$$

For $(\varphi - \phi_{a-a',b-b'}) \in (\pi/2, 3\pi/2)$, we close the contour integration in the lower complex plane, where there is

another singularity located at $-q_\omega = -k_\omega(1+i\alpha_G/2)$, leading to

$$\begin{aligned}\int_{-\infty}^{\infty} dk \frac{e^{ikr_{a-a',b-b'}\cos\left(\varphi-\phi_{a-a',b-b'}\right)}|k|g^2(k,\varphi)}{\omega-\omega_k+i\delta_m} &= 2\pi i\frac{|-k_\omega|}{-v_{k_\omega}}g^2(-k_\omega,\varphi)e^{-iq_\omega r_{a-a',b-b'}\cos\left(\varphi-\phi_{a-a',b-b'}\right)}\\ &= -2\pi i\frac{|k_\omega|}{v_{k_\omega}}g^2(k_\omega,\varphi-\pi)e^{-iq_\omega r_{a-a',b-b'}\cos\left(\varphi-\phi_{a-a',b-b'}\right)}\\ &= -2\pi i\frac{k_\omega}{v_{k_\omega}}g^2(k_\omega,\varphi-\pi)e^{iq_\omega r_{a-a',b-b'}\cos\left(\varphi-\pi-\phi_{a-a',b-b'}\right)}.\end{aligned} \tag{S25}$$

When $\phi_{a-a',b-b'}\in[-\pi/2,\pi/2)$, we divide the integral region $\varphi\in[0,\pi]$ into two parts $[0,\phi_{a-a',b-b'}+\pi/2]$ and $(\phi_{a-a',b-b'}+\pi/2,\pi]$, and calculate Eq. (S22) as

$$\begin{aligned}&\frac{L_yL_z}{(2\pi)^2}\sum_{a',b'}\int_0^{\phi_{a-a',b-b'}+\frac{\pi}{2}}d\varphi\int_{-\infty}^{\infty}dk\frac{e^{ikr_{a-a',b-b'}\cos\left(\varphi-\phi_{a-a',b-b'}\right)}|k|g^2(k,\varphi)}{\omega-\omega_k+i\delta_m}\hat{\beta}_{a',b'}\\ &+\frac{L_yL_z}{(2\pi)^2}\sum_{a',b'}\int_{\phi_{a-a',b-b'}+\frac{\pi}{2}}^{\pi}d\varphi\int_{-\infty}^{\infty}dk\frac{e^{ikr_{a-a',b-b'}\cos\left(\varphi-\phi_{a-a',b-b'}\right)}|k|g^2(k,\varphi)}{\omega-\omega_k+i\delta_m}\hat{\beta}_{a',b'}\\ &=-i\frac{L_yL_z}{2\pi}\sum_{a',b'}\int_0^{\phi_{a-a',b-b'}+\frac{\pi}{2}}d\varphi\frac{k_\omega}{v_{k_\omega}}g^2(k_\omega,\varphi)e^{iq_\omega r_{a-a',b-b'}\cos\left(\varphi-\phi_{a-a',b-b'}\right)}\hat{\beta}_{a',b'}\\ &-i\frac{L_yL_z}{2\pi}\sum_{a',b'}\int_{\phi_{a-a',b-b'}+\frac{\pi}{2}}^{\pi}d\varphi\frac{k_\omega}{v_{k_\omega}}g^2(k_\omega,\varphi-\pi)e^{iq_\omega r_{a-a',b-b'}\cos\left(\varphi-\pi-\phi_{a-a',b-b'}\right)}\hat{\beta}_{a',b'}\\ &=-i\frac{L_yL_z}{2\pi}\sum_{a',b'}\left(\int_0^{\phi_{a-a',b-b'}+\frac{\pi}{2}}d\varphi+\int_{\phi_{a-a',b-b'}-\frac{\pi}{2}}^{0}d\varphi\right)\frac{k_\omega}{v_{k_\omega}}g^2(k_\omega,\varphi)e^{iq_\omega r_{a-a',b-b'}\cos\left(\varphi-\phi_{a-a',b-b'}\right)}\hat{\beta}_{a',b'}\\ &=-i\frac{L_yL_z}{2\pi}\sum_{a',b'}\int_{\phi_{a-a',b-b'}-\frac{\pi}{2}}^{\phi_{a-a',b-b'}+\frac{\pi}{2}}d\varphi\frac{k_\omega}{v_{k_\omega}}g^2(k_\omega,\varphi)e^{iq_\omega r_{a-a',b-b'}\cos\left(\varphi-\phi_{a-a',b-b'}\right)}\hat{\beta}_{a',b'}.\end{aligned} \tag{S26}$$

The same calculation applies when $\phi_{a-a',b-b'}\in[\pi/2,3\pi/2)$. So via changing the integral domain of φ in Eq. (S22), we arrive at

$$\begin{aligned}&\sum_{a'\neq a\ \text{or}\ b'\neq b}\sum_{\mathbf{k}}\frac{e^{i\left[(a-a')k_y\Lambda_y+(b-b')k_z\Lambda_z\right]}}{\omega-\omega_k+i\delta_m}g_{\mathbf{k}}^2\hat{\beta}_{a',b'}\\ &=\left(-i\frac{L_yL_z}{2\pi}\right)\sum_{a'\neq a\ \text{or}\ b'\neq b}\int_{\phi_{a-a',b-b'}-\frac{\pi}{2}}^{\phi_{a-a',b-b'}+\frac{\pi}{2}}d\varphi\frac{k_\omega}{v_{k_\omega}}g^2(k_\omega,\varphi)e^{iq_\omega r_{a-a',b-b'}\cos\left(\varphi-\phi_{a-a',b-b'}\right)}\hat{\beta}_{a',b'}.\end{aligned} \tag{S27}$$

Using the on-shell approximation $\omega\to\Omega$, the matrix elements of the effective Hamiltonian of the magnons in the nanomagnet read

$$\begin{aligned}\mathcal{H}_{\text{eff}}\big|_{a=a',b=b'} &= \Omega-i\delta_\beta-i\Gamma(\mathbf{r}_{a-a',b-b'}=0),\\ \mathcal{H}_{\text{eff}}\big|_{a\neq a'\ \text{or}\ b\neq b'} &= -i\Gamma(\mathbf{r}_{a-a',b-b'}\neq 0),\end{aligned} \tag{S28}$$

where the effective coupling between magnons within the nanomagnets

$$\Gamma(\mathbf{r}_{a-a',b-b'}=0)=\frac{L_yL_z}{4\pi}\int_0^{2\pi}d\varphi\frac{k_\Omega}{v_{k_\Omega}}g^2(k_\Omega,\varphi), \tag{S29}$$

and in different nanomagnets

$$\Gamma(\mathbf{r}_{a-a',b-b'}\neq 0)=\frac{L_yL_z}{2\pi}\int_{\phi_{a-a',b-b'}-\frac{\pi}{2}}^{\phi_{a-a',b-b'}+\frac{\pi}{2}}d\varphi\frac{k_\Omega}{v_{k_\Omega}}g^2(k_\Omega,\varphi)e^{iq_\Omega r_{a-a',b-b'}\cos\left(\varphi-\phi_{a-a',b-b'}\right)}. \tag{S30}$$

IV. PRECISE TOPOLOGICAL CHARACTERIZATION FOR ONE-DIMENSION

The analytical solution for the frequency spectra of long-range coupled magnons exists in the one-dimension [2], which allows a comparison with the numerical results that we model by the periodic boundary condition. We consider a finite-sized array of N CoFeB magnetic nanowires that are equally spaced on the YIG substrate with neighboring distance L_0. According to Ref. [2], the elements of the effective Hamiltonian matrix $\mathcal{H}_{\text{eff}}|_{ll'} = (1 - i\tilde{\alpha}_G)\Omega\delta_{ll'} - i\Gamma_{ll'}$, in which the effective coupling between the l-th and l'-th wire

$$\Gamma_{ll'} = \begin{cases} (\Gamma_L + \Gamma_R)/2, & l = l' \\ \Gamma_L e^{iq_\Omega|l-l'|L_0}, & l > l' \\ \Gamma_R e^{iq_\Omega|l-l'|L_0}, & l < l' \end{cases}, \tag{S31}$$

where Γ_L and Γ_R are the coupling strength between the magnons from the left to the right (the right to the left) wire, and $q_\Omega = k_\Omega(1 + i\alpha_G/2)$ with the resonant wave number k_Ω of the substrate magnon to the FMR frequency Ω of the wire. The analytical solution for the frequency spectra reads [2]

$$\omega_\kappa = (1 - i\tilde{\alpha}_G)\,\Omega - i\frac{\Gamma_L}{2}\frac{1 + e^{i(q_\Omega+\kappa)L_0}}{1 - e^{i(q_\Omega+\kappa)L_0}} + i\frac{\Gamma_R}{2}\frac{1 + e^{i(\kappa-q_\Omega)L_0}}{1 - e^{i(\kappa-q_\Omega)L_0}}. \tag{S32}$$

For the periodic system, $\kappa L_0 \in [0, 2\pi]$ is real.

On the other hand, we can numerically calculate the frequency spectra in the periodic system constructed according to our approach as addressed in the main text, where the effective coupling in the open system Eq. (S31) is replaced by the periodic one

$$\Gamma^p_{ll'} = \sum_n \Gamma_{l(l'+nN)},$$

where summation runs over the integer $n \in (-\infty, +\infty)$. As an example, we consider the array of $N = 100$ CoFeB nanowires of thickness $d = 30$ nm and width $w = 100$ nm spaced equally with neighboring distance $L_0 = 1$ μm on the thin YIG film of thickness $s = 10$ nm, biased by the in-plane applied magnetic field $\mu_0 H_0 = 0.05$ T. The saturated magnetization of CoFeB wire $\mu_0\tilde{M}_s = 1.6$ T is pinned along the wire $\hat{\mathbf{z}}$-direction due to the shape anisotropy, in which configuration the FMR frequency $\Omega = 2\pi \times 21.2$ GHz. For the YIG substrate, its saturated magnetization $\mu_0 M_s = 0.177$ T, Gilbert damping coefficient $\alpha_G = 10^{-3}$, and exchange stiffness $\alpha_{\text{ex}} = 3 \times 10^{-16}$ m^2. The resonant wave number of magnon in YIG to Ω is $k_\Omega = 1.13 \times 10^8$ m^{-1}. We numerically diagonalize the periodic Hamiltonian matrix $\mathcal{H}^p_{\text{eff}}|_{ll'} = (1 - i\tilde{\alpha}_G)\Omega\delta_{ll'} - i\Gamma^p_{ll'}$, and compare the eigenfrequencies, relative to $(1 - i\tilde{\alpha}_G)\Omega$, with the analytical solution (S32) with different chiralities as shown in Fig. S3. The eigenfrequency is normalized by $\Gamma_a = (\Gamma_{\text{L}} + \Gamma_{\text{R}})/2$. All the numerically calculated frequency spectra locate at the curves from the analytical calculation. Such excellent agreement validates our numerical approach.

[1] M. Küß, M. Heigl, L. Flacke, A. Hörner, M. Weiler, M. Albrecht, and A. Wixforth, Nonreciprocal Dzyaloshinskii–Moriya Magnetoacoustic Waves, Phys. Rev. Lett. **125**, 217203 (2020).

[2] T. Yu and B. W. Zeng, Giant microwave sensitivity of a magnetic array by long-range chiral interaction driven skin effect, Phys. Rev. B **105**, L180401 (2022).

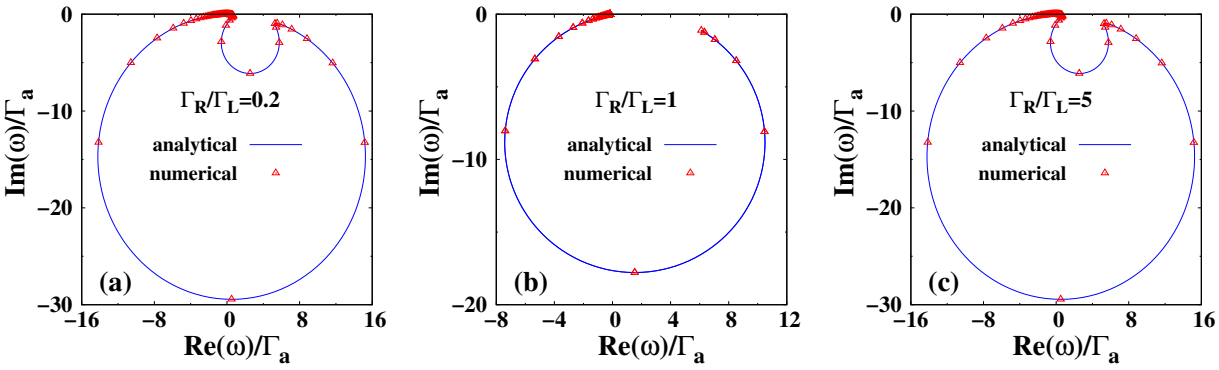

FIG. S3. Comparison of frequency spectra in the one-dimensional system from the analytical and numerical calculations with different chiralities $\Gamma_{\mathrm{R}}/\Gamma_{\mathrm{L}} = 0.2$ [(a)], 1 [(b)], and 5 [(c)].